J. Biochem. **141,** 855–866 (2007)
doi:10.1093/jb/mvm093

Chimeric Structural Stabilities in the Coiled-Coil Structure of the NECK Domain in Human Lectin-Like Oxidized Low-Density Lipoprotein Receptor 1 (LOX-1)

Tomoko Ishigaki[1], Izuru Ohki[1], Naoko Utsunomiya-Tate[2] and Shin-icih Tate[1,3,*,†]

[1]Department of Structural Biology, Biomolecular Engineering Research Institute (BERI), 6-2-3, Furuedai, Suita, Osaka 565-0874; [2]Research Institute of Pharmaceutical Science, Musashino University, 1-1-20 Shinmachi Nishitokyo-shi, Tokyo 202-8585; and [3]PRESTO, Japan Science and Technology Agency (JST), 4-1-8 Honcho Kawaguchi, Saitama, Japan

Received February 25, 2007; accepted March 30, 2007; published online April 6, 2007

LOX-1 (lectin-like oxidized low-density lipoprotein receptor 1) is the major oxidized LDL (OxLDL) receptor on endothelial cells. The extracellular part of LOX-1 comprises an 82-residue stalk region (NECK) and a C-type lectin-like ligand-binding domain (CTLD). The NECK displays sequence similarity to the coiled-coil region of myosin, having been suggested it adopts a rod-like structure. In this article, we report the structural analyses of human LOX-1 NECK using a variety of approaches including limited proteolysis, chemical cross-linking, circular dichroism (CD) and NMR. Our analysis reveals a unique structural feature of the LOX-1 NECK. Despite significant sequence similarity with the myosin coiled-coil, LOX-1 NECK does not form a uniform rod-like structure. Although not random, one-third of the N-terminal NECK is less structured than the remainder of the protein and is highly sensitive to cleavage by a variety of proteases. The coiled-coil structure is localized at the C-terminal part of the NECK, but is in dynamic equilibrium among multiple conformational states on a μs–ms time scale. This chimeric structural property of the NECK region may enable clustered LOX-1 on the cell surface to recognize OxLDL.

Key words: atherosclerosis, LDL, membrane proteins, CD, NMR.

Abbreviations: CD, circular dichroism; CTLD, C-type lectin-like ligand-binding domain; DC-SIGN, dendritic cell-specific ICAM-3 grabbing nonintegrin; DTT, dithiothreitol; HSQC, heteronuclear single quantum coherence spectroscopy; LDL, low-density lipoprotein; MALDI-TOF, matrix-assisted laser desorption ionization time-of-flight; MS, mass spectrometry; NMR, nuclear magnetic resonance; SDS–PAGE, sodium dodecyl sulphate polyacrylamide gel electrophoresis.

Lectin-like oxidized LDL (OxLDL) receptor 1 (LOX-1) is the major OxLDL receptor found on endothelial cells (*1*, *2*). LOX-1 mediates the internalization of OxLDL into cells and can induce endothelial cell dysfunction that is believed to constitute an early step in the development of atherosclerosis (*3*–*5*). LOX-1 expression is up-regulated in pathological conditions affecting the vasculature, including hypertension, diabetes and atherosclerosis (*6*). The expression of LOX-1 enhances a variety of intracellular processes that lead to expression of adhesion molecules, to which inflammatory cells attach, and endothelial activation, which affects a variety of gene expression such as endothelial constitutive nitric oxide synthase (eNOS) and monocyte chemoattractant protein 1 (MCP-1) (*3*, *5*, *7*–*9*). Immunostaining shows that the most prominent expression of LOX-1 occurs in the endothelial cells in atherosclerotic lesions (*10*, *11*). Taken together these results indicate that LOX-1 plays a critical role in endothelial dysfunction and injury, which lead to initiation and progression of atherosclerosis.

LOX-1 is a membrane protein with a type II orientation consisting of four domains (Fig. 1A): a short cytoplasmic domain, single transmembrane domain, a stalk region (also called the NECK domain) and a C-type lectin-like domain (CTLD) that binds to the ligands. On the cell surface, LOX-1 exists as a homodimer linked by an inter-chain disulphide bond at C140 (Fig. 1A) (*12*). We have reported the crystal structure of human LOX-1 CTLD solved as a homodimer linked by the disulphide bond in the short NECK domain attached to the CTLD (*13*, *14*). Analysis of the structure revealed that the LOX-1 CTLD dimer surface possesses a characteristic arrangement of basic residues, which we referred to as the 'basic spine' (*13*). *In vivo* experiments using LOX-1 mutants expressed on the CHO cell surface have suggested that maintaining the basic spine structure on the CTLD dimer is essential for the binding of LOX-1 to OxLDL (*13*). Based on the crystal structure of the ligand-binding domain of LOX-1, together with the *in vivo* ligand-binding experiments, we proposed the LOX-1 binding mode to OxLDL (*13*).

*To whom correspondence should be addressed. Department of Mathematical and Life Sciences, Graduate School of Science, Hiroshima University, 1-3-1 Kagamiyama, Higashi-Hiroshima 739-8526, Japan. Tel: +81-82-424-7387, Fax: +81-82-424-7387, E-mail: tate@hiroshima-u.ac.jp
†Present address: Department of Mathematical and Life Sciences, Graduate School of Science, Hiroshima University, 1-3-1 Kagamiyama, Higashi-Hiroshima 739-8526, Japan.

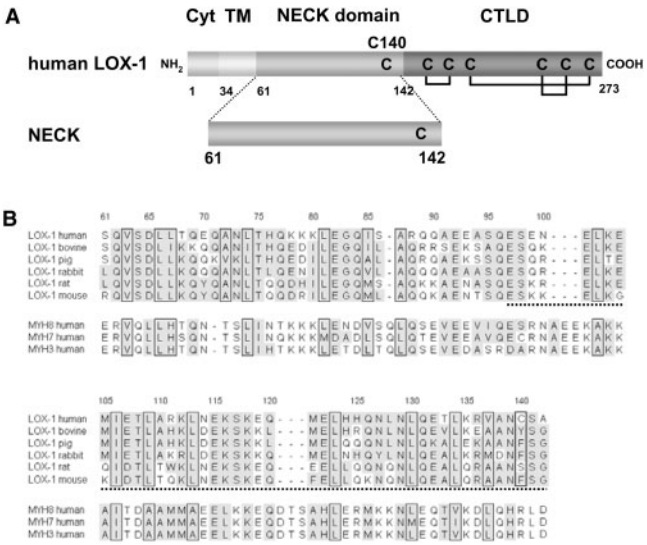

Fig. 1. **Amino acid sequence of the NECK domain.** (A) Schematic drawing of the overall domain structure of LOX-1; Cyt: cytoplasmic domain, TM: transmembrane domain, NECK: neck domain, CTLD: C-type lectin-like domain. The isolated NECK fragment used in the present work is denoted by NECK, which comprises residues 61–142. (B) Comparison of the amino acid sequence of the NECK domain among LOX-1 orthologs. The sequences are also compared with those of different myosin heavy chains. The dotted underline indicates the sequence that corresponds to the 46-amino-acid repeat unit, which is one of the triple repeat units found in rat LOX-1.

LOX-1 is a member of the C-type lectin-like protein family, which is classified into evolutionary group V (*15*). Members of natural killer cell (NK-cell) receptor family, which are encoded in a specific gene region known as the natural killer gene complex, are classified into this group (*16*). Proteins in this group share the domain architecture that comprises the NECK domain and CTLD in the extracellular regions (*15*). Members of the evolutionary group V protein family display a high level of sequence conservation in the CTLD, but only a limited sequence similarity in the NECK domain, although they all retain coiled-coil sequence character (*15*, *17*).

The coiled-coil is a prevailing oligomerization motif in proteins (*18*). It is also known to be a highly versatile folding motif; small variations in sequence lead to a remarkable diversity in oligomerization states (*18–20*). The sequence variation found in the coiled-coil NECK domains among the C-type lectin-like proteins in group V may reflect the specific function of each member protein. It is known that different coiled-coil sequences result in different assemblies of the ligand-binding domains for dendritic cell-specific ICAM-3 grabbing nonintegrin (DC-SIGN) (*21*) and Mannose-binding protein (MBP) (*22*), both of which are the members of the C-type lectin-like family of proteins. DC-SIGN forms a tetramer through a coiled-coil stalk that consists of a series of seven and a half tandem repeats of a highly conserved sequence of 23 amino acids (*21*). MBP is a trimer comprising a collagen-like NECK of a parallel triple-stranded coiled-coil of α-helices (*22*). The different assemblies induced by the NECK are closely related to the specific function of each protein. Accordingly, the LOX-1 NECK, which possesses a different sequence from that of DC-SIGN or MBP, presumably plays a specific functional role during LOX-1 ligand recognition.

In this article, we report the structure analysis of the LOX-1 NECK using a variety of different methods including limited proteolysis, chemical cross-linking, circular dichroism (CD) and NMR. Our studies revealed that the LOX-1 NECK is made up of two structurally distinctive compartments with different stabilities; one-third of the N-terminal portion is highly flexible but not a random coil, whereas the remaining C-terminal region forms a coiled-coil structure. However, the C-terminal coiled-coil is rather unstable and is in dynamic equilibrium among multiple conformational states. The unique NECK structure of LOX-1 is likely to play a significant function in the binding of LOX-1 to OxLDL. Based on the proposed LOX-1 ligand-binding mode to OxLDL (*13*), the possible role of the LOX-1 NECK is discussed.

MATERIALS AND METHODS

Expression and Purification of LOX-1 NECK Fragments—Human LOX-1 cDNA from aortic endothelial cell (HAEC) was a kind gift of Dr Sachiko Machida (National Food Research Institute, Tsukuba, Japan). The DNA fragment encoding the LOX-1 NECK domain (residues 61–142) was cloned into pET28a (Novagen, Madison, WI) at the NcoI and NdeI sites. The recombinant protein included an N-terminal His_6-tag sequence followed by a PreScission Protease (Amersham Pharmacia Biotech, Piscataway, NJ) cleavage recognition site. Thus, four residues (GPHM) of vector encoded sequence were included at the N-terminus of the tag cleaved recombinant protein. Because the NECK domain contains no aromatic residues, a GGY sequence was added to the C-terminal region in order to facilitate convenient monitoring of the protein concentration. The NECK fragment used for the NMR experiments possesses a tyrosine residue just prior to the NECK sequence. The C140S amino acid replacement was carried out on the NECK fragment using the Stratagene QuickChange kit (La Jolla, CA). The N-terminal deletion mutant NECK-C, comprising residues 89–142, was also cloned into pET28a at the NcoI and NdeI sites. Purification of the wild-type and C140S mutant NECK fragments, and their respective N-terminal truncated versions, were all carried out in the same way. *Escherichia coli* strain BL21(DE3) cells (Stratagene) harbouring the corresponding plasmid to express the NECK fragment were grown at 37°C in M9 minimal medium containing kanamycin (50 μg/ml). Heterologous gene expression was induced at an $A_{600} = 0.5$ by the addition of isopropyl-β-D-thiogalactopyranoside to a final concentration of 1 mM for 4 h at 37°C. The cells were harvested by centrifugation (5000 rpm for 5 min). The cell pellet from a 1.0 liter culture, typically about 3 g wet weight, was resuspended in 50 ml buffer solution (20 mM Tris–HCl pH 7.5, 300 mM NaCl) containing a protease inhibitor mixture (Roche Applied Science, Basel, Switzerland), and then lysed

by sonication (ASTRASON, Farmingdale, NY) on ice. After centrifugation (15,000 rpm for 30 min), the supernatant from the lysate was collected and directly loaded onto a HisTrap HP (Amersham Pharmacia Biotech) affinity column equilibrated with Ni^{2+} at 4°C. After sample loading, the column was washed with 50 ml 10 mM imidazole solution (50 mM Tris–HCl, pH 7.5, 400 mM NaCl), followed by a further wash with 25 ml imidazole solution. The NECK fragment was eluted with 50 ml 300 mM imidazole solution. The eluted fractions containing the NECK fragment were pooled (30 ml) and subjected to the tag cleavage reaction by adding 300 μl PreScission protease (2 units/μl). The cleavage reaction was performed at 4°C overnight. The solution containing PreScission protease was applied to a GSTrap (1 ml volume) and HisTrap (1 ml volume) column sequentially to remove the protease and cleaved His_6-tag fragment from the solution. The flow-through containing the recombinant protein was collected and ammonium sulphate added to give a final concentration of 0.8 M. The solution was then applied to a HiTrap-Phenyl HP (Amersham Pharmacia Biotech) column and fractionation was performed using a linear gradient of ammonium sulphate from 0.8 to 0 M in 20 mM Tris–HCl pH 7.2 containing 0.4 M NaCl. The collected fractions were analysed by sodium dodecyl sulphate polyacrylamide gel electrophoresis (SDS–PAGE) using a 17.5% acrylamide gel. The pooled fractions containing the NECK fragment were 75% saturated by ammonium sulphate to collect the target protein. The solution was stored at 4°C overnight and the precipitate was then collected by centrifugation (15,000 rpm for 30 min). The precipitate was dissolved in 5 ml buffer solution (20 mM citrate, pH 4.0, 0.4 M NaCl) and then applied to a Sephadex 75 (26/60) gel filtration column equilibrated in the same buffer. Fractions containing the NECK fragment were identified by SDS–PAGE analysis (17.5% gel). The yield for the NECK fragment was typically 5 mg of purified protein from 1.0 liter culture.

Limited Proteolysis—Proteolysis was performed at 20°C in a solution containing 50 mM Tris–HCl pH 8.0, 0.5 mg/ml NECK fragment and various concentrations of protease. In the present analyses, we used trypsin (Promega, Madison, WI) and α–chymotrypsin (Sigma-Aldrich, St Louis, MO). The weight-to-weight ratios for the NECK fragment and protease were varied between 1:0.1, 1:0.01 and 1:0.001. The volume of the sample solution was 10 μl. After 30 min incubation at 20°C, the reaction was quenched by the addition of 2 μl 1% trifluoroacetic acid. The stopped reaction mixture was subjected to both matrix-assisted laser desorption ionization time-of-flight (MALDI-TOF) mass spectrometry (MS) and SDS–PAGE (15% gel) analyses. Fragments isolated from the SDS–PAGE gel were subjected to N-terminal sequence analyses.

MALDI-TOF MS—Spectra were acquired on a MALDI-TOF mass spectrometer (Voyager, Applied Biosystems, Foster City, CA) equipped with a 337 nm nitrogen laser, using a 20 kV extraction voltage and a time-delayed extraction. A mixture of saturated 3,5-dimethoxy-4-hydroxycinnamic acid (Sigma-Aldrich) in 33% acetonitrile and 0.1% trifluoroacetic acid was used as the matrix. The proteolytic digestion mixture was dried and dissolved in 5 μl of 80% acetonitrile and 0.1% trifluoroacetic acid for analysis. The fragment solutions were mixed on a plate with the matrix in a 1:1 ratio and dried at room temperature prior to measuring mass spectra. Insulin chain B and myoglobin were used as external standards for the molecular mass calibration.

Chemical Cross-link Analysis—The NECK fragment solution (0.45 mg/ml in 20 mM sodium-/potassium–phosphate buffer pH 7.0, containing 400 mM NaCl) was used for the chemical cross-linking experiment using BS3 [bis(sulphosuccinimidyl)suberate; Pierce, Rockford, IL]. The BS3 concentration in the reaction solution varied between 0.1, 0.2, 0.4, 0.8, 1.6, 3.2, 6.4 and 12.8 mM. After the reaction at room temperature for 1 h, the content of the cross-linked protein component was monitored by SDS–PAGE (15% gel).

Circular Dichroism Spectrometry—CD spectra of the NECK fragments were measured on a J-720 spectropolarimeter (Jasco, Easton, MD) at 20°C. Four different sample conditions were used; 20 mM citrate buffer, pH 4.0, including 100 or 400 mM NaCl for acidic conditions and 10 mM sodium phosphate, pH 7.0 and 100 or 400 mM NaCl for neutral conditions. Protein concentration was kept to 20 μM in all CD experiments. Sample solutions were placed in a fused silica cell (1 mm path length), and 36 scans were averaged. The fractional percentage of α-helical content was calculated from $[\theta]_{222}$ as described previously (*23*).

N-terminal Sequencing—The N-terminal amino acid sequences of the fragments were determined by automated Edman degradation using an Applied Biosystems 492 pulsed liquid phase sequencer equipped with an on-line 785A phenylthiohydantoin derivative analyzer.

NMR Spectroscopy—The uniformly ^{15}N- or $^{15}N/^{13}C$-labelled NECK fragments were obtained from the *E. coli* cells expressing the fragment grown in M9 minimal medium culture containing $^{15}NH_4Cl$ with or without [U-^{13}C]glucose. The purified proteins were concentrated to give 170 μl of 0.2 to 1.0 mM sample solution. Sample buffer solution used for the resonance assignment experiments was 20 mM citrate, pH 4.0, containing 400 mM NaCl (5% D_2O content for NMR frequency lock). In the experiments for accessing the dimer states, the solution comprising 20 mM Tris–HCl pH 7.2, and 400 mM NaCl was used. The sample solution was packed into a microcell (Shigemi Co. Ltd, Tokyo, Japan) for NMR measurements.

Two-dimensional ^1H-^{15}N heteronuclear single quantum coherence (HSQC) spectra and a set of three-dimensional triple resonance NMR spectra were acquired at 298 K on Bruker (Karlsruhe, Germany) 750 or 600 MHz NMR spectrometers. To obtain the resonance assignments for the backbone ^1H, ^{15}N, $^{13}C\alpha$, $^{13}C\beta$ and $^{13}C'$ nuclei, the following spectra were used: HNCO, HNCA, HN(CO)CA, HNCACB and CBCA(CO)NH. All data were processed with the program NMRPipe (*24*) and the observed peaks were subsequently picked by the PIPP program package (*25*). The resultant peak tables were subjected to an in-house, semiautomatic backbone resonance assignment program JASS (Java script-based graphical backbone resonance assignment tool), to accelerate the backbone

resonance assignment process. The ^{1}H chemical shifts were referenced indirectly to external 2,2-dimethyl-2-silapentane-5-sulphonic acid (DSS) as 0.0 ppm. Zero frequencies for ^{13}C and ^{15}N chemical shifts were derived from the experimentally obtained ^{1}H frequency for DSS by multiplying the relative frequencies by 0.251449530 and 0.101329118, respectively (*26*).

For the backbone resonance assignment of LOX-1 CTLD consisting of residues 143–273, ^{15}N- and $^{15}N/^{13}C$-labelled CTLD fragments were used, which were prepared according to the procedure described in our previous work (*13*). The NMR experiments were done for the sample solution containing 0.5 mM of protein in 100 mM acetate buffer, pH 3.8, at 310 K. A standard set of triple resonance spectra were used for the assignment. The assignment process was done in the same way as described earlier.

Analysis of the Dimer States of the NECK Fragment by NMR—The ^{15}N-labelled NECK fragment was dissolved in 20 mM Tris–HCl pH 7.2 and 400 mM NaCl to a final protein concentration of 0.2 mM. ^{1}H-^{15}N HSQC spectra were measured at 298 K on a Bruker 750 MHz spectrometer. For the analysis of the reduced state of the NECK structure, dithiothreitol (DTT) was added to the sample solution up to a concentration of 10 mM to cleave the inter-chain disulphide bond. To make up the random structural state of the NECK domain, 200 mM guanidium chloride was added to the sample solution containing 10 mM DTT. After adding DTT and guanidium chloride, the solution was adjusted to pH 7.2.

RESULTS

Oligomerization State of the NECK—The recombinant NECK fragment formed a stable disulphide-linked dimer during purification, which was revealed by SDS–PAGE analysis of the NECK fragment in reduced and non-reduced protein preparations (Fig. 2A). In a series of chemical cross-linking experiments, using various concentrations of BS3 against a fixed amount of NECK fragment (0.45 mg/ml), it was shown there was no higher order protein assemblies over dimer (Fig. 2B).

Previous chemical cross-linking experiments using LOX-1 expressed on CHO cell surface have shown that LOX-1 forms, at least, a hexamer on the cell surface (*12*). However, the present result demonstrates that hexamer formation is not mediated by the NECK.

Limited Proteolysis to the NECK—Limited proteolysis was performed to identify the structured parts in the NECK. Cleavage by trypsin or α-chymotrypsin produced discrete fragments (Fig. 3A). The smallest fragment showing resistance to trypsin cleavage was assigned to the region comprising residues 89–142 by MS and N-terminal sequence analyses (Fig. 3B). The smallest region resistant to α-chymotrypsin digestion comprised residues 75–142 (Fig. 3B). Medium-sized fragments generated by tryptic cleavage comprised residues, 81–142 and 80–142 (Fig. 3B). Partial α-chymotrypsin cleavage also gave a mid-sized fragment made up of residues 68–143 (Fig. 3B). The limited proteolysis experiments consistently showed the region of the NECK comprising residues 61–88 to be protease-sensitive.

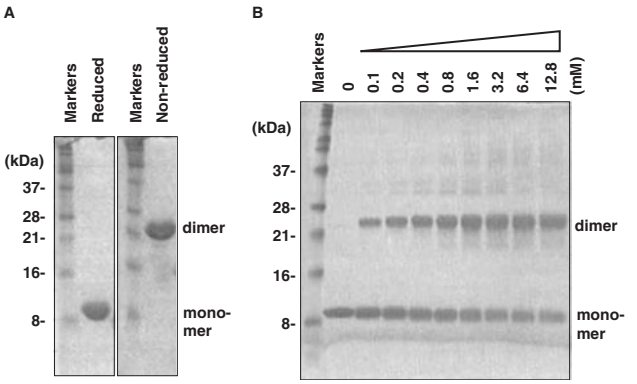

Fig. 2. **Oligomerization state of the NECK fragment.** (A) The purified NECK fragment was analysed by SDS–polyacrylamide gel electrophoresis with and without β-mercaptoethanol treatment. (B) NECK fragment (0.45 mg/ml) was incubated with various concentrations (top row, in mM) of the cross-linker BS3 for 1 h at room temperature and analysed by SDS–PAGE. The position of molecular weight marker proteins are shown on the left, and the assignment of monomer and dimer positions are on the right.

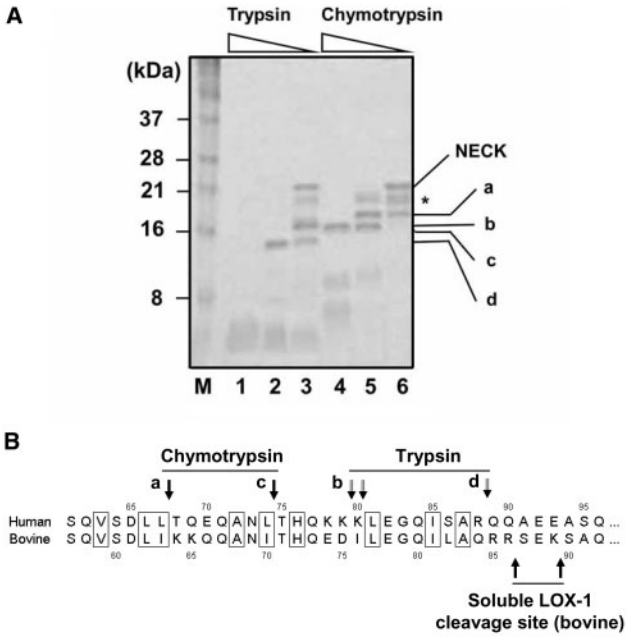

Fig. 3. **Limited proteolysis of the NECK fragment.** (A) Effect of trypsin and chymotrypsin concentration on the digestion of NECK. The NECK fragment was digested with increasing amounts of protease. The weight-to-weight ratio of NECK to protease was 1:0.1, 1:0.01 and 1:0.001 (from left to right) for each protease; lanes 2–4 for trypsin, and lanes 5–7 for α-chymotrypsin. Lane 1 shows SDS–PAGE analysis of the isolated NECK fragment used for the limited proteolysis experiments. The band indicated by an asterisk was generated by adventitious proteolysis during purification of the NECK fragment. (B) The identification of the scissile bond was determined by N-terminal sequence analysis of each proteolytic product (a–d in Fig. 3A). For fragment b, due to the clustering of lysine residues, two possible cleavage sites were identified. The cleavage sites identified for the soluble form of bovine LOX-1 (*29*) are shown with the corresponding sequence of human LOX-1 protease sensitive NECK region. The smeary band marked by an asterisk contained a mixture of various cleavage fragments that could not be clearly analysed.

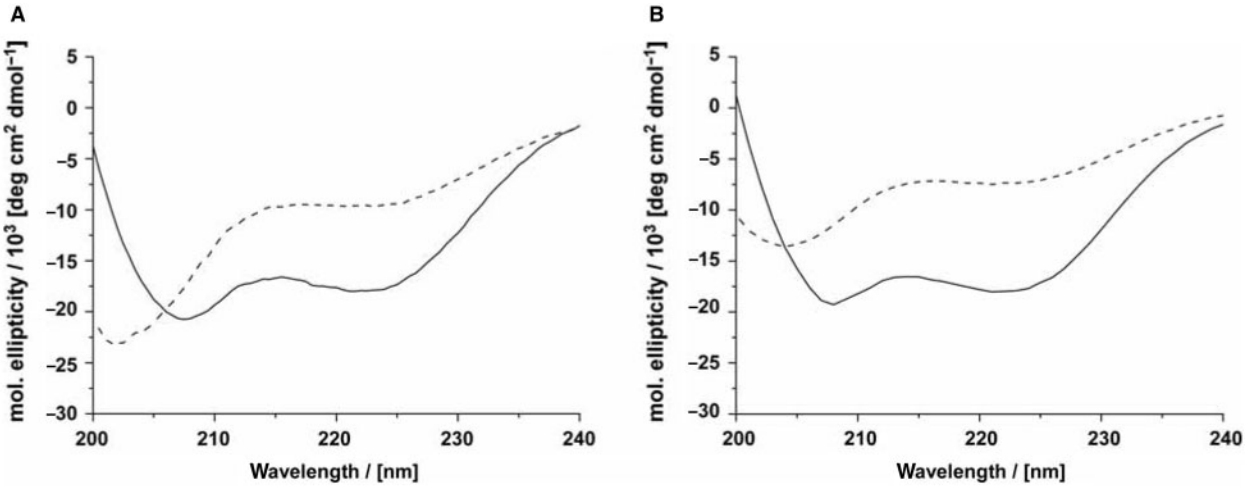

Fig. 4. **CD spectra of LOX-1 NECK and NECK-C fragments.** (A) Comparison of the CD spectra for the NECK (solid line) and NECK(C140S) (dotted line) fragments at pH 7.0 and 0.1 M NaCl concentration. (B) CD spectra for the NECK-C (solid line) and NECK-C(C140S) (dotted line) at pH 7.0 and 0.1 M NaCl concentration.

The N-terminal one-third of the NECK is, therefore, less structured than the remaining part of the NECK.

It is interesting to note that the minimal protease-resistant region, residues 89–142, of the human LOX-1 NECK largely corresponds to the repeating sequence found in the rat LOX-1 NECK (Fig. 1B). Rat LOX-1 NECK domain has three repeating homologous sequences, whilst bovine and human LOX-1 contain only one corresponding repeating unit; each unit consists of 46 amino acid residues rich in Glu, Gln, Leu and Lys (*27*). Because of the insertion of two repeating sequence units, the total length of rat LOX-1 NECK is longer than that of the human protein (*27*). The observed protease resistance of the region comprising a repeating unit in human LOX-1 NECK domain suggests that the repeating unit may function as a common scaffold in the NECK among LOX-1 orthologs.

We address another relating observation to the minimal protease resistant region in the human LOX-1 NECK. Cell-surface LOX-1 is known to be cleaved by some proteases that are associated with the plasma membrane (*28*, *29*). The cleavage sites that generate the soluble form of LOX-1 were identified for bovine LOX-1, which shows high sequence similarity to the human protein (i.e. 71.3% identity and 88.4% similarity) (*29*). Interestingly, the protease cleavage sites in the soluble form of bovine LOX-1 are almost coincident with the N-terminal site for the minimal protease resistant fragment in human LOX-1 (Fig. 3B). *In vivo* observations of the soluble form of LOX-1 indicate that the NECK comprises distinctive regions with different structural stabilities, which is consistent with the present results obtained for human LOX-1 NECK.

Structural Characterization of the NECK by CD—Ultraviolet CD spectroscopy was used to elucidate the secondary structure of the NECK. The NECK displays similar ellipticity minima at 208 and 222 nm, characteristic of α-helical coiled-coil structures for helix forming peptides (Fig. 4A). The $[\theta]_{222}/[\theta]_{208}$ ratios observed under various conditions are listed in Table 1. Because the n–π^* transition (222 nm) is mainly indicative of the α-helical content, whereas the π–π^* transition (208 nm) polarizes parallel to the helix axis, the ellipticity ratio $[\theta]_{222}/[\theta]_{208}$ is used as an indicator for the occurrence of α-helical coiled-coil structure; $[\theta]_{222}/[\theta]_{208}$ ratio of 1.0 is expected for a stable coiled-coil (*30*, *31*). Only minor changes were observed in the $[\theta]_{222}/[\theta]_{208}$ ratios and helicities for the NECK under the applied conditions (Table 1), demonstrating that hydrophobic interactions and salt bridges are not effective in maintaining the NECK coiled-coil structure, whilst the inter-chain disulphide bond is crucial.

By using the C140S mutant, we elucidated the structural role of the disulphide bond in the NECK. The CD spectrum for the NECK(C140S) was compared with that for the wild-type (Fig. 4A). Loss of the disulphide bond resulted in a drastic reduction of fractional helix content and $[\theta]_{222}/[\theta]_{208}$ ratio (Table 1). The NECK coiled-coil structure is severely destabilized by the loss of the inter-chain disulphide bond. Furthermore, NECK(C140S) displays a significant CD spectral change upon varying the pH and ionic strength, in contrast to the disulphide-linked NECK (Table 1). The results show that the single inter-chain disulphide bond extends α-helical coiled-coil structure in the NECK. The role of the disulphide bond is analogous to that of the 'trigger sequence', which extends α-helical coiled-coil structure (*32*).

The structural properties of the NECK protease resistant region (residues 89–142) was explored using the NECK fragment comprising residues 89–142, NECK-C. The CD spectra for NECK and NECK-C in 0.1 M NaCl, pH 7.0 were compared (Fig. 4A and B). The NECK-C showed a larger $[\theta]_{222}/[\theta]_{208}$ ratio compared to that for the NECK (Table 1). This indicates that the coiled-coil region is localized to the C-terminal part of the NECK (Fig. 4B). The loss of the inter-chain disulphide bond consistently resulted in reduced helix content and $[\theta]_{222}/[\theta]_{208}$ ratio in NECK-C, as found in the CD spectrum for NECK-C(C140S) (Fig. 4B).

Table 1. **Mean molar ellipticities at 202 nm and 222 nm, fractional helix content, and ratio for the ellipticities $[\theta]_{222}/[\theta]_{208}$.**

Experiments[a]	$[\theta]_{208/10}{}^3$ deg cm^2 dmol^{-1}	$[\theta]_{222/10}{}^3$ deg cm^2 dmol^{-1}	Helicity[b] (estimated residues in helix)	$[\theta]_{222}/[\theta]_{208}$
NECK [NaCl 0.4 M, pH4.0]	−20.9	−18.1	0.46 (41)	0.87
NECK [NaCl 0.1 M, pH4.0]	−20.7	−17.9	0.46 (41)	0.87
NECK [NaCl 0.4 M, pH7.0]	−20.1	−17.2	0.44 (39)	0.86
NECK [NaCl 0.1 M, pH7.0]	−20.7	−17.9	0.46 (41)	0.87
NECK(C140S) [NaCl 0.4 M, pH4.0]	−18.2	−12.4	0.32 (29)	0.68
NECK(C14SS) [NaCl 0.1 M, pH4.0]	−17.7	−11.6	0.30 (27)	0.66
NECK(C140S) [NaCl 0.4 M, pH7.0]	−20.0	−7.9	0.20 (18)	0.54
NECK(C140S) [NaCl 0.1 M, pH7.0]	−16.8	−9.6	0.25 (22)	0.57
NECK-C [NaCl 0.4 M, pH4.0]	−22.5	−20.7	0.53 (32)	0.92
NECK-C [NaCl 0.1 M, pH4.0]	−20.9	−19.5	0.50 (31)	0.94
NECK-C [NaCl 0.4 M, pH7.0]	−20.0	−18.7	0.48 (29)	0.94
NECK-C [NaCl 0.1 M, pH7.0]	−19.3	−18.0	0.46 (28)	0.93
NECK-C(C140S) [NaCl 0.4 M, pH4.0]	−14.8	−10.4	0.27 (17)	0.70
NECK-C(C140S) [NaCl 0.1 M, pH4.0]	−13.9	−9.5	0.24 (15)	0.68
NECK-C(C140S) [NaCl 0.4 M, pH7.0]	−10.2	−6.3	0.16 (10)	0.61
NECK-C(C140S) [NaCl 0.1 M, pH7.0]	−11.5	−7.4	0.19 (12)	0.64

[a]NECK denotes the NECK fragment containing full domain (residues 61–142). NECK-C denotes the C-terminal part of the NECK domain (residues 89–142), determined by limited proteolysis. [b]Experimental fractional helix contents determined from mean molar ellipticities at 222 nm at 20°C with a protein concentration of 20 μM.

NMR Analysis of the NECK—To further characterize the NECK structure, we performed NMR analysis of the NECK fragment at pH 4.0 in 0.4 M NaCl, which condition ensures the most stable coiled-coil structure as elucidated by the CD spectra (Table 1). The number of the cross peaks clearly observed in the ^{1}H-^{15}N HSQC spectrum for the NECK was much less than expected; we anticipated 87 backbone correlation signals but only 38 appeared in the spectrum (Fig. 5A). The observed backbone signals were assigned using standard triple resonance NMR data sets (Fig. 5A); the assigned amide ^{1}H, ^{15}N, ^{13}Cα, ^{13}Cβ and carbonyl carbon chemical shifts are available as supplemental data (Supplementary Table S-1). Most of the assigned ^{1}H-^{15}N correlation signals came from the N-terminal protease sensitive regions and the short part in the C-terminal edge (Fig. 5B). The remaining unassigned residues showed severely broadened signals with limited signal intensities, which prohibited their resonance assignments (Fig. 5C). The result suggests that the protease resistant coiled-coil region is presumably in conformational exchange among multiple conformational states on a μs–ms timescale (Fig. 5C) (*33*). Thus, although the LOX-1 NECK C-terminal region is relatively protease resistant, it does not adopt a stable rod-like structural unit. The C-terminal region is also flexible in a different manner from the N-terminus.

NMR Analyses of the NECK in Various States—To further corroborate the structural dynamics of the NECK, we compared the ^{1}H-^{15}N HSQC spectra for the NECK in the presence and absence of DTT (Fig. 6A and B). Because the optimal pH for the reduction by DTT is in the rage from 7.1 to 8.0, we performed the experiments in the neutral pH condition, pH 7.2. Three additional isolated cross peaks were observed in the ^{1}H-^{15}N HSQC spectrum at pH 7.2, which were overlapped to other peaks in the spectra at pH 4.0 (Figs. 5A and 6A). The span for the unassigned region in the NECK was not essentially altered by the pH change in the presence of the disulphide bond, being consistent with the CD data (Table 1). The cleavage of the inter-chain disulphide bond increased the number of signals in the ^{1}H-^{15}N HSQC spectrum (Fig. 6B). The result demonstrates that the loss of the disulphide bond facilitates conformational exchange and structural flexibility of the NECK coiled-coil part. Note that the sample pH was readjusted to 7.2 after the addition of DTT so that the spectral change excluded any pH-related effects. The NMR observation is consistent with the reduced helix content for the NECK(C140S) revealed by the CD spectra (Table 1). Loss of the inter-chain disulphide bond reduces the structural stability of the protein and, thus, increases the number of sharp NMR signals. Analysis of the ^{1}H-^{15}N HSQC spectrum of the NECK lacking a disulphide bond shows that 17 signals are still difficult to observe. The corresponding residues are located on the residual helix region, which is engaged in conformational equilibrium on an intermediate NMR chemical shift time scale, typically in the μs–ms time range (Fig. 6B). A CD spectrum of NECK(C140S) at neutral pH shows that the fragment retains 20% helical content, corresponding to 18 residues (Table 1). The estimated number of residues in the helix is in good agreement with the number of broadened NMR signals for the NECK observed under reducing conditions.

We observed 78 signals on the ^{1}H-^{15}N HSQC spectrum for the NECK under extremely denaturing conditions (10 mM DTT and 200 mM guanidium chloride, where the pH was readjusted to pH 7.2) (Fig. 6C). The number of observed signals is still less than anticipated (87 signals), probably due to signal overlap caused by limited signal dispersion. Taken together, the severely broadened NMR signals for the NECK in the native state suggest that the coiled-coil part is in conformational equilibrium on an NMR timescale imposing signal broadening. Most probably, the equilibrium is among the multiple

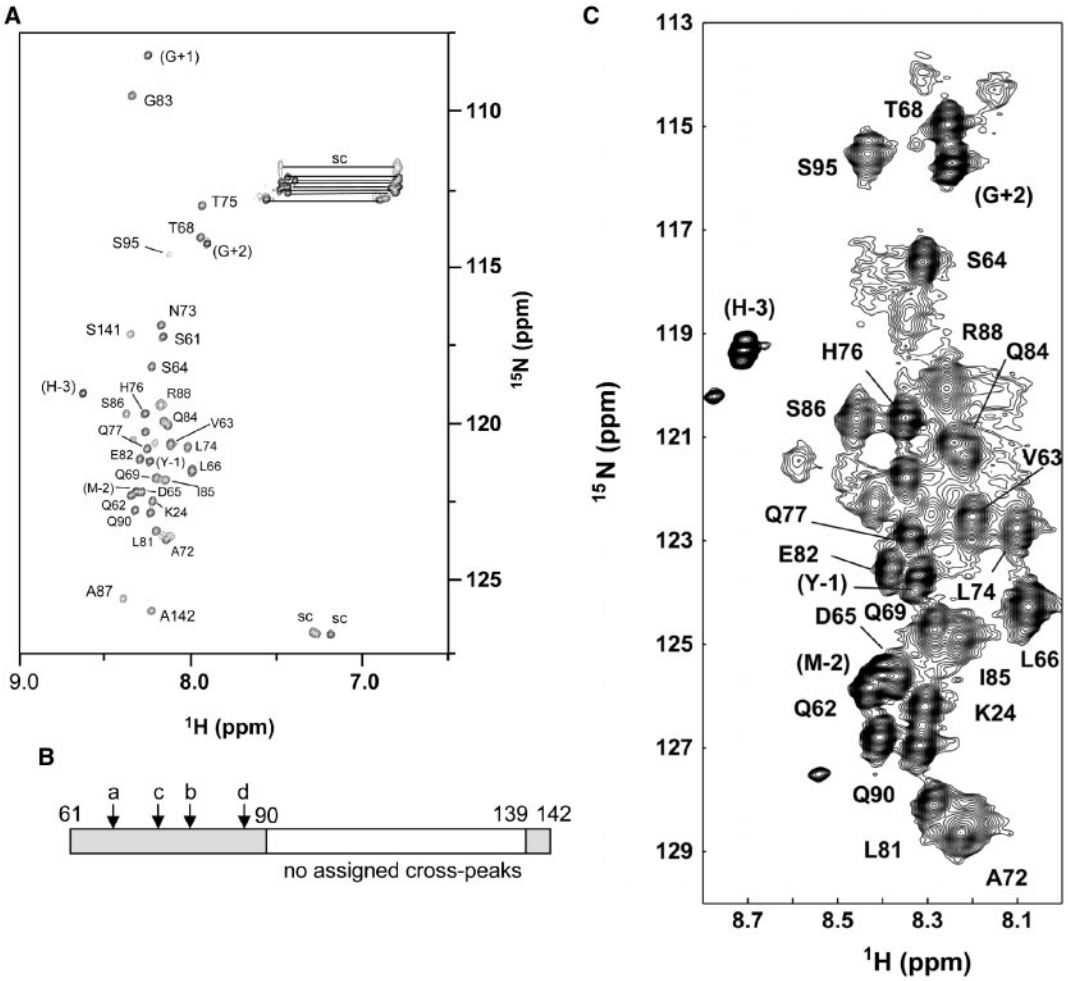

Fig. 5. **^{1}H-^{15}N HSQC spectrum for the NECK fragment.** (A) Backbone resonance assignments are shown on the spectrum. Sc indicates the signals from side chain atoms including GLN and ASN side chain NH_2 and ARG $N^{\varepsilon}H$, which are not assigned in the present analysis. The spectrum was measured for the ^{15}N-labelled NECK fragment at pH 4.0 and 0.4 M NaCl at 298 K. (B) Location of the assigned residues is indicated on the NECK domain; the residues in gray shade were assigned and the residues in the region indicated by a white box were not assigned due to their severe signal broadening. (C) Close-up view of a part of the ^{1}H-^{15}N HSQC spectrum for the NECK with lower threshold to plot weak NMR signals. Unassigned signals were seen as severely broadened correlation peaks.

conformational states, which may explain the extreme broadening observed on the spectrum for the disulphide-linked NECK (Fig. 5A).

DISCUSSION

Chimeric Coiled-coil Structure of the LOX-1 NECK—The present work has shown that the human LOX-1 NECK domain has a chimeric coiled-coil structure, which comprises a less-structured N-terminal region and a C-terminal coiled-coil region that is in dynamic conformational equilibrium among multiple conformational states.

The sequences of α-helical coiled-coils are known to be characterized by a heptad repeat of seven residues, denoted **a** to **g**, with a 3, 4 hydrophobic repeat of mostly apolar amino acids at positions **a** and **d** (*34*, *35*). Two-stranded coiled-coil structures are stabilized by the hydrophobic interface between the α-helices, where two apolar residues in the '**a**' and '**d**'-positions interlock in a 'knob-into-hole' fashion by the winding of helices around one another (*20*, *36*). The overall unstable nature of the coiled-coil structure in LOX-1 NECK domain seems to be explained from its sequence; no clear heptad repeat can be found in the NECK (Fig. 1B). Although two seven-residue fragments that contain apolar residues in the first (**a**) and fourth (**d**) positions are present [V62(**a**)-L66(**d**)-Q69 and L102(**a**)-M105(**d**)-T108], these two regions are separated and cannot cooperatively form a coiled-coil structure.

Careful inspection of the N-terminal NECK sequence gives another structural insight. In the N-terminal part, there are three consecutive seven-residue repeats having glutamine residue at the '**d**'-position; L66(**a**)-Q69(**d**)-A72, one-residue insertion (N73) and L74(**a**)-Q77(**d**)-K80, L81(**a**)-Q84(**d**)-A87. The heptad repeats having glutamine at the '**d**'-positions are found in the unstable coiled-coil region of the scallop myosin rod, which can adopt two

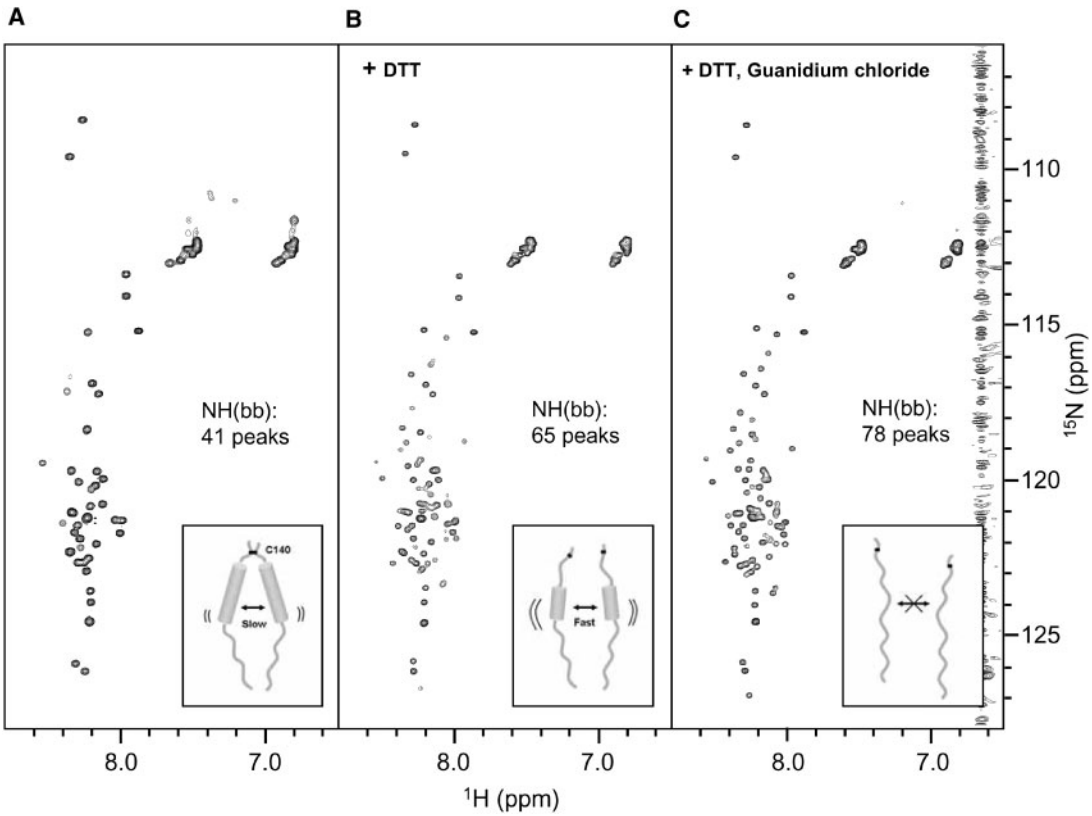

Fig. 6. **Comparison of ^{1}H-^{15}N HSQC spectra for the NECK fragments under various conditions.** A: NECK with an inter-chain disulphide bond at pH 7.2, 0.4 M NaCl. B: NECK in the presence of 10 mM DTT. C: NECK in the presence of 10 mM DTT and 200 mM guanidium chloride as denaturant. Insets; schematic images of the NECK conformational exchange are given under each experimental condition.

different dimer structures in the asymmetric crystal unit (*37*). In each dimer of the scallop myosin rod, the '**d**'-position glutamine (Q849) residues pack in a different fashion; only one of the side chains forms a 'knob-into-hole' contact with the opposite helix, and the other side chain is oriented towards the solvent (*37*). Indeed, X-ray crystal studies produced a poor density map of the N-terminal residues of the scallop myosin rod structure (*37*), indicating that the N-terminal region is structurally unstable. Asymmetrically packed glutamine residues are also found at the boundary between the coiled-coil and non-coiled-coil regions of tropmyosin (*38*). These X-ray results support the present observation that the N-terminal LOX-1 NECK is less structured due to the variant heptad repeats having a '**d**'-position glutamine.

Despite of the less-structured properties observed in the present analyses, the N-terminal part of LOX-1 NECK is not a random coil. Some of the assigned amide protons in the N-terminal region of the NECK have shown clear sequential NH(i)-NH(i + 1) NOEs (Fig. S1), which strongly suggest that these connected residues experience an α-helical conformation that maintain neighbouring NH protons in spatial proximity to allow significant magnetization transfer. Due to limited signal dispersion in the NH dimension we could not observe the entire sequential NOE connectivity for all the N-terminal residues giving clear HSQC signals. However, the observation of some clear NH(i)-NH(i + 1) NOEs provides evidence that the protease-sensitive N-terminal region may transiently fold into an α-helical structure, possibly forming a two-stranded coiled-coil as anticipated from the sequence properties.

In the C-terminal coiled-coil region, the inter-chain disulphide bond was shown to be effective in extending the coiled-coil structure. The role of the disulphide bond is apparently related to that of the 'trigger sequence'. The 'trigger sequence', comprising a short segment of residues, is known to extend a parallel two-stranded α-helical coiled-coil structure (*32*, *39*). Indeed, a stable coiled-coil structure is not formed by the heptad repeat alone, but also requires the trigger sequence. The trigger sequence typically comprises 13 residues with limited sequence variations; the consensus sequence is xxLExchxcxccx (x: any residue, h: hydrophobic residue, c: charged residue) (*32*). The NECK sequence of LOX-1 does not contain a trigger sequence. The present observation that the NECK extends the coiled-coil in the presence of the inter-chain disulphide bond suggests that the inter-chain disulphide bond functions to 'zip up' the coiled-coil dimer as the trigger sequence does (Fig. 6A and B insets). The triggering effect does not appear to extend as far as the N-terminal part of the protein, which contains the variant heptad repeats having intrinsically unstable structural property.

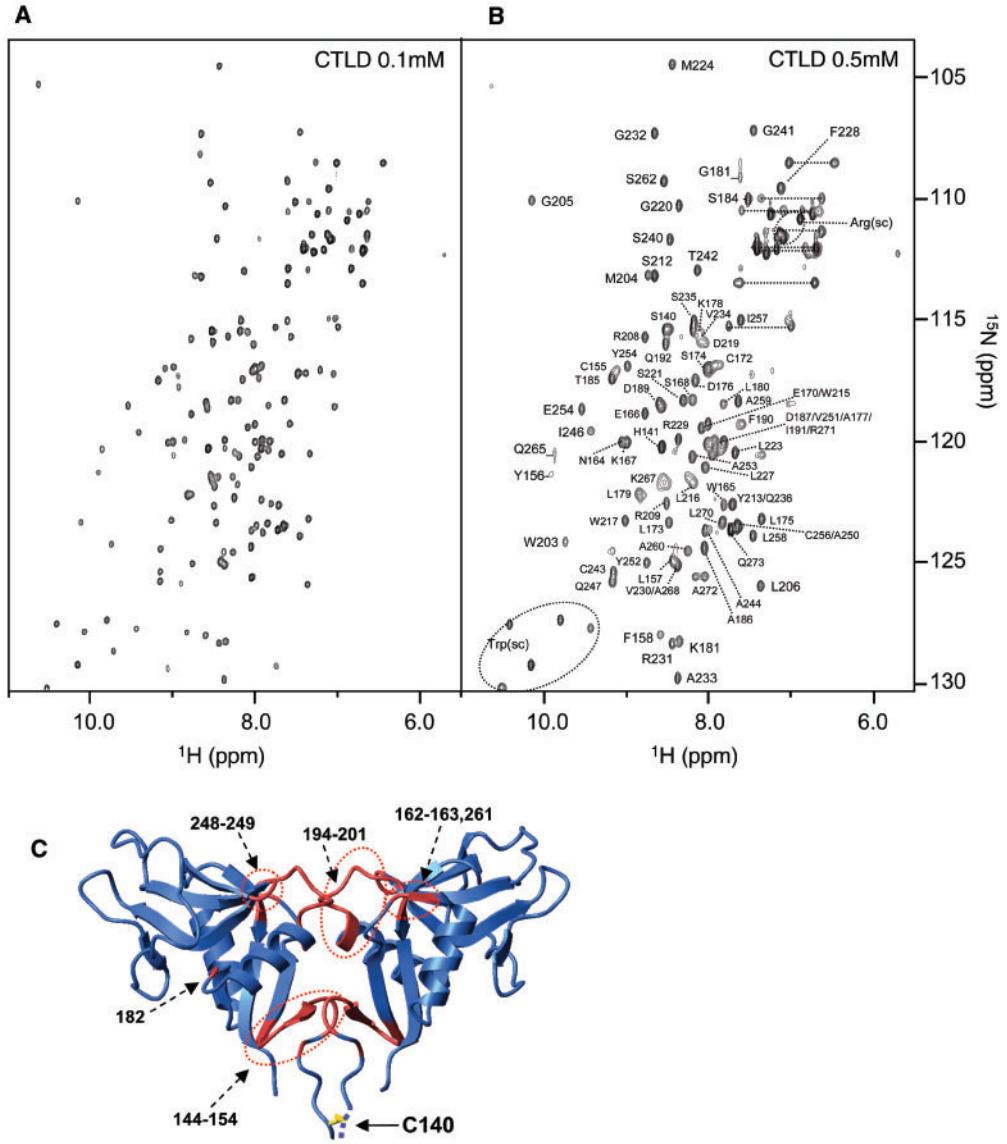

Fig. 7. **Concentration-dependent spectral changes in the ^{1}H-^{15}N HSQC spectrum for human LOX-1 CTLD.** (A) ^{15}N-labelled CTLD at 0.1 mM concentration. (B) ^{15}N-labelled CTLD at 0.5 mM concentration, with backbone resonance assignments obtained under the same conditions. (C) The residues that were not assigned due to severe signal broadening are marked in red on the CTLD dimer structure (PDB accession code: 1YXK) (*13*).

Structural and Functional Significance of the Disulphide Bond in the NECK—Previous studies have shown that loss of the inter-chain disulphide bond in LOX-1 does not affect the binding activity for OxLDL on the cell surface (*12*). However, the present work has shown that the lack of the disulphide bond destabilizes the NECK coiled-coil structure, which may cause the disruption of the proper dimer arrangement of the CTLD; the proper dimer arrangement of the CTLD is shown to be essential for the ligand binding (*13*). This apparently contradictory observation suggests that the other part of the protein may exert a complimentary function to the disulphide bond in the intact LOX-1.

We have shown by analytical ultracentrifugation experiments that the LOX-1 CTLD (residues 143–273, not including the disulphide bond at C140) behaves as a monomer in solution at low protein concentration (50 μM) (*13*). To further investigate the state of the CTLD in solution, we compared the ^{1}H-^{15}N HSQC spectra for the ^{15}N-labelled CTLD at two different protein concentrations (Fig. 7A and B). It should be noted that the CTLD used in these experiments does not contain C140. The NMR spectrum for CTLD at 0.1 mM protein concentration showed clear signals with apparently equal intensities. By comparison, however, the spectrum for 0.5 mM CTLD shows that some of the signals have become broadened and/or disappeared (Fig. 7A and B). The reduction in signal intensities due to the broadening can be ascribed to an exchange between the dimer and monomer states of CTLD on a μs–ms time scale.

The noted observation is that the residues showing missing and/or broadened signals map to the dimer interface of the CTLD crystal structure (Fig. 7C) (*13*). The concentration-dependent spectral changes infer that CTLD autonomously associates to a specific dimer as found in the crystal structure at higher protein concentration (Fig. 7C).

LOX-1 is known to form a cluster on the cell surface (*12*), which achieves a local condensation of the protein. Under the condition, CTLD should autonomously associate to form a specific dimer, thereby presumably zipping up the coiled-coil structure at the C-terminal part of the NECK in the absence of the inter-chain disulphide bond. The induced NECK coiled-coil may synergistically stabilize the dimer arrangement of the CTLDs. This could explain the marginal functional role of the disulphide bond in LOX-1 on the cell surface, despite it being essential for coiled-coil formation in the isolated NECK fragment.

The Biological Significance of the Chimeric Coiled-coil Structure of the LOX-1 NECK Domain—A notable feature of the LOX-1 NECK domain is that it consists of distinct coiled-coil structures showing different stabilities (Fig. 8A). Chemical cross-linking of LOX-1 expressed in CHO cells has shown that the protein forms at least a hexamer on the cell surface, which comprises three homodimeric forms of LOX-1 (*12*). Comparison of the size of the CTLD dimer surface (70 Å) with the diameter of low-density lipoprotein (LDL) (250 Å), estimated by electron microscopy, suggests the hexamerically clustered LOX-1 may be an ideal size for interaction with an LDL particle (Fig. 8B) (*13*, *40*).

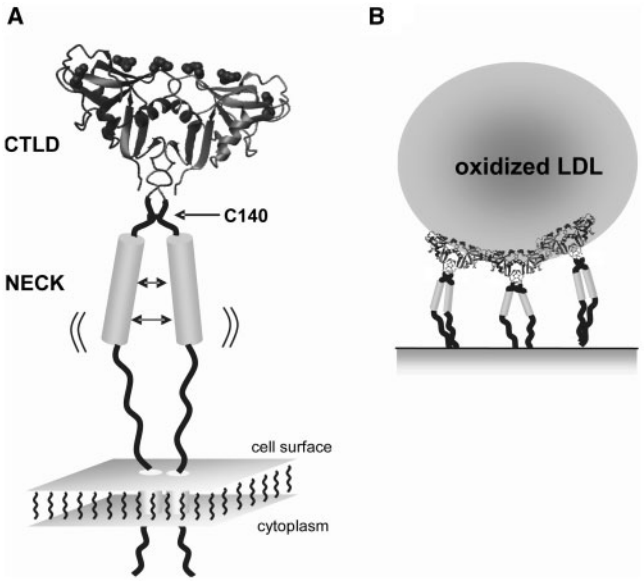

Fig. 8. **Schematic representation of LOX-1 on the cell surface.** (A) Human LOX-1 is anchored on the cell surface by the unstable coiled-coil structure and unstructured part of the NECK, which allows free precession of the ligand-binding domain, CTLD, to seek out the binding sites on OxLDL. We hypothesize that the LOX-1 binding sites are the repeating amphipathic helices that expose a negatively charged surface, based on the proposed LDL structural model (*40*). (B) LOX-1 forms a hexamer, which consists of three dimers, on the cell surface (*12*). Clustered LOX-1 binds to the amphipathic helices on the LDL surface by flexibly adjusting the CTLD orientation against OxLDL using the flexible structure of the NECK domain.

There is a paucity of structural data for LDL, which consists of lipids and a single polypeptide component of apolipoprotein B-100 (apoB-100), comprising about 4500 residues that wraps around the lipid particle. Sequence analysis of apoB-100 indicates that there are clusters of amphipathic α helices on the LDL surface (*40*). The approximate number of amphipathic α helices has been estimated to range from 51 to 65 according to the subclass of LDL (*40*). Further sequence analysis of apoB-100 has revealed the presence of nine repeated amphipathic helical regions consisting of a 22-residue consensus sequence (*41*). The consensus sequence, DFIDEFNEKLKDLSDQLNDFLN, forms the amphipathic α-helix that exposes negatively charged residues to the solvent (*13*). Based on sequence analysis of apoB-100, we previously proposed the mode of interaction of LOX-1 with OxLDL (*13*). Our analysis indicated that the LOX-1 dimer surface, which harbours the basic spine, recognizes a negatively charged amphipathic helix of apoB100 on the LDL surface. Thus, LOX-1 proteins in the hexameric cell surface cluster simultaneously interact with OxLDL at multiple amphipathic helices on the LDL particle.

The apparent affinity of LOX-1 on the cell surface for OxLDL was estimated to have a $Kd = 1.7 \times 10^{-8}$ M (*5*). We have recently conducted surface plasmon resonance (SPR) experiments which show that a single LOX-1 dimer has a much lower affinity for OxLDL (*K*d in the order of 10^{-5} M) compared with LOX-1 clustered on the SPR sensor (*K*d in the order of 10^{-10} M) (Ohki, I. *et al*., in preparation). These results suggest that the clustering of LOX-1 on the cell surface is essential for multiple-site binding to OxLDL to gain binding specificity. LOX-1 proteins within the cluster on the cell surface must locate binding sites on the OxLDL particle, comprising amphipathic helices with negative surface charges. During this process, the flexible NECK structure may facilitate the necessary interactions (Fig. 8A and B). The flexible NECK structure in LOX-1 probably plays an analogous role to the unstable coiled-coil region in smooth muscle myosin 'head-rod junction', where a flexible region around the junction is required for optimal mechanical performance (*37*, *42*).

In the present study the LOX-1 NECK, *per se*, was not shown to form higher order assemblies over the disulphide-linked dimer. The CTLD does not form higher order protein assemblies (*13*). The LOX-1 cluster formation on the cell surface (*12*) is not mediated by an intrinsic property of LOX-1 protein. Other factors must be engaged in the LOX-1 clustering.

The well-characterized receptor assembly found for the DC-SIGN, another member of the CTLD protein family, may be related to the LOX-1 assembly process. DC-SIGN forms a NECK-mediated tetramer but its higher-order assembly, over tetramer, on the cell surface is essential for the DC-SIGN function; randomly distributed tetrameric DC-SIGNs on the cell do not capture virus-sized particles (*43*). It is shown that DC-SIGN forms an

assembly in the lipid-raft, a cholesterol enriched patch on the cell membrane, which limits lateral diffusion of the receptor on the cell surface. We think, thus, that LOX-1 cluster is also mediated by the lipid-raft on the cell surface.

In conclusion, the present work has revealed that the human LOX-1 NECK domain possesses a chimeric coiled-coil structure. Specifically, the NECK domain comprises a flexible N-terminal coiled-coil region that transiently folds and a more stable coiled-coil part at the C-terminus, which is in dynamics equilibrium among multiple conformational states on a μs–ms time scale (Fig. 8A). It is remarkable that the LOX-1 NECK does not form a rod-like uniform coiled-coil as anticipated from its overall sequence similarity to the coiled-coil part of the myosin heavy chain. The unique NECK structure of LOX-1 may facilitate efficient binding of the LOX-1 clustering on the cell surface to multiple binding sites on OxLDL particle, which are made up of amphipathic repeating helices in apoB100 (*13*). Thus, the NECK domain instigates specific interactions between the clustered receptors on the cell and the OxLDL particle (Fig. 8B). We have shown that the clustering of LOX-1 is not mediated by the intrinsic property of LOX-1. Based on the preceding finding for DC-SIGN, which shows lipid-raft mediates the receptor clustering on the cell (*43*), LOX-1 clustering may also be facilitated by the lipid-raft in the cell membrane. According to the concentration-dependent NMR signal changes for the LOX-1 CTLD (Fig. 7), the CTLD was shown to autonomously form the specific dimer as found in the crystal structure (*13*). The CTLD, thus, should stabilize the NECK coiled-coil dimer and synergistically the CTLD dimer itself by zipping up the NECK coiled-coil region, whose role being comparable for the inter-chain disulphide bond solely found in the human NECK among LOX-1 orthologs. This autonomous dimerization of the LOX-1 CTLD under the condensed state, as in the cluster on the cell surface, may explain the discrepant *in vivo* observation, which shows the marginal functional significance of the disulphide bond in the human LOX-1 NECK expressed on the cell (*12*).

Supplementary data are available at *JB* online.

This work was supported by the Japan New Energy and Industrial Technology Development Organization (NEDO). S.T. thanks for the financial support from the Japan Science and Technology Agency, PRESTO. S.T. also appreciates the financial support from Hiroshima University for achieving a part of the work. A part of this research was also supported by MEXT.HAITEKU (2004–2008).

REFERENCES

1. Chen, M., Masaki, T., and Sawamura, T. (2002) LOX-1, the receptor for oxidized low-density lipoprotein identified from endothelial cells: implications in endothelial dysfunction and atherosclerosis. *Pharmacol. Ther.* **95**, 89–100
2. Sawamura, T., Kume, N., Aoyama, T., Moriwaki, H., Hoshikawa, H., Aiba, Y., Tanaka, T., Miwa, S., Katsura, Y., Kita, T., and Masaki, T. (1997) An endothelial receptor for oxidized low-density lipoprotein. *Nature* **386**, 73–77
3. Kita, T. (1999) LOX-1, a possible clue to the missing link between hypertension and atherogenesis. *Circ. Res.* **84**, 1113–1115
4. Kita, T., Kume, N., Minami, M., Hayashida, K., Murayama, T., Sano, H., Moriwaki, H., Kataoka, H., Nishi, E., Horiuchi, H., Arai, H., and Yokode, M. (2001) Role of oxidized LDL in atherosclerosis. *Ann. N.Y. Acad. Sci.* **947**, 199–206
5. Mehta, J.L. (2004) The role of LOX-1, a novel lectin-like receptor for oxidized low density lipoprotein, in atherosclerosis. *Can. J. Cardiol.* **20** (Suppl. B), 32B–36B
6. Kume, N., Murase, T., Moriwaki, H., Aoyama, T., Sawamura, T., Masaki, T., and Kita, T. (1998) Inducible expression of lectin-like oxidized LDL receptor-1 in vascular endothelial cells. *Circ. Res.* **83**, 322–327
7. Mehta, J.L., Li, D.Y., Chen, H.J., Joseph, J., and Romeo, F. (2001) Inhibition of LOX-1 by statins may relate to upregulation of eNOS. *Biochem. Biophys. Res. Commun.* **289**, 857–861
8. Mehta, J.L., Hu, B., Chen, J., and Li, D. (2003) Pioglitazone inhibits LOX-1 expression in human coronary artery endothelial cells by reducing intracellular superoxide radical generation. *Arterioscler. Thromb. Vasc. Biol.* **23**, 2203–2208
9. Moriwaki, H., Kume, N., Kataoka, H., Murase, T., Nishi, E., Sawamura, T., Masaki, T., and Kita, T. (1998) Expression of lectin-like oxidized low density lipoprotein receptor-1 in human and murine macrophages: upregulated expression by TNF-alpha. *FEBS Lett.* **440**, 29–32
10. Kakutani, M., Ueda, M., Naruko, T., Masaki, T., and Sawamura, T. (2001) Accumulation of LOX-1 ligand in plasma and atherosclerotic lesions of Watanabe heritable hyperlipidemic rabbits: identification by a novel enzyme immunoassay. *Biochem. Biophys. Res. Commun.* **282**, 180–185
11. Kataoka, H., Kume, N., Miyamoto, S., Minami, M., Moriwaki, H., Murase, T., Sawamura, T., Masaki, T., Hashimoto, N., and Kita, T. (1999) Expression of lectinlike oxidized low-density lipoprotein receptor-1 in human atherosclerotic lesions. *Circulation* **99**, 3110–3117
12. Xie, Q., Matsunaga, S., Niimi, S., Ogawa, S., Tokuyasu, K., Sakakibara, Y., and Machida, S. (2004) Human lectin-like oxidized low-density lipoprotein receptor-1 functions as a dimer in living cells. *DNA Cell Biol.* **23**, 111–117
13. Ohki, I., Ishigaki, T., Oyama, T., Matsunaga, S., Xie, Q., Ohnishi-Kameyama, M., Murata, T., Tsuchiya, D., Machida, S., Morikawa, K., and Tate, S. (2005) Crystal structure of human lectin-like, oxidized low-density lipoprotein receptor 1 ligand binding domain and its ligand recognition mode to OxLDL. *Structure. (Camb.)* **13**, 905–917
14. Park, H., Adsit, F.G., and Boyington, J.C. (2005) The 1.4 angstrom crystal structure of the human oxidized low density lipoprotein receptor lox-1. *J. Biol. Chem.* **280**, 13593–13599
15. Drickamer, K. and Dodd, R.B. (1999) C-Type lectin-like domains in Caenorhabditis elegans: predictions from the complete genome sequence. *Glycobiology* **9**, 1357–1369
16. Yokoyama, W.M. and Plougastel, B.F. (2003) Immune functions encoded by the natural killer gene complex. *Nat. Rev. Immunol.* **3**, 304–316
17. Drickamer, K. (1999) C-type lectin-like domains. *Curr. Opin. Struct. Biol.* **9**, 585–590
18. Burkhard, P., Stetefeld, J., and Strelkov, S.V. (2001) Coiled coils: a highly versatile protein folding motif. *Trends Cell Biol.* **11**, 82–88
19. Cohen, C. and Parry, D.A. (1990) Alpha-helical coiled coils and bundles: how to design an alpha-helical protein. *Proteins* **7**, 1–15
20. Lupas, A. (1996) Coiled coils: new structures and new functions. *Trends Biochem. Sci.* **21**, 375–382
21. Bernhard, O.K., Lai, J., Wilkinson, J., Sheil, M.M., and Cunningham, A.L. (2004) Proteomic analysis of DC-SIGN

on dendritic cells detects tetramers required for ligand binding but no association with CD4. *J. Biol. Chem.* **279**, 51828–51835
22. Weis, W.I. and Drickamer, K. (1994) Trimeric structure of a C-type mannose-binding protein. *Structure.* **2**, 1227–1240
23. Chakrabartty, A., Schellman, J.A., and Baldwin, R.L. (1991) Large differences in the helix propensities of alanine and glycine. *Nature* **351**, 586–588
24. Delaglio, F., Grzesiek, S., Vuister, G.W., Zhu, G., Pfeifer, J., and Bax, A. (1995) NMRPipe: a multidimensional spectral processing system based on UNIX pipes. *J. Biomol. NMR* **6**, 277–293
25. Garrett, D.S., Powers, R., Gronenborn, A.M., and Clore, G.M. (1991) A common sense approach to peak picking in two-, three-, and fourdimensional spectra using automatic computer analysis of contour diagrams. *J. Magn. Reson.* **95**, 214–220
26. Markley, J.L., Bax, A., Arata, Y., Hilbers, C.W., Kaptein, R., Sykes, B.D., Wright, P.E., and Wüthrich, K. (1998) Recommendations for the presentation of NMR structures of proteins and nucleic acids IUPAC-IUBMB-IUPAB Inter-Union Task Group on the Standardization of Data Bases of Protein and Nucleic Acid Structures Determined by NMR Spectroscopy. *J. Biomol. NMR* **12**, 1–23
27. Nagase, M., Hirose, S., and Fujita, T. (1998) Unique repetitive sequence and unexpected regulation of expression of rat endothelial receptor for oxidized low-density lipoprotein (LOX-1). *Biochem. J.* **330** (Pt 3), 1417–1422
28. Kume, N. and Kita, T. (2001) Roles of lectin-like oxidized LDL receptor-1 and its soluble forms in atherogenesis. *Curr. Opin. Lipidol.* **12**, 419–423
29. Murase, T., Kume, N., Kataoka, H., Minami, M., Sawamura, T., Masaki, T., and Kita, T. (2000) Identification of soluble forms of lectin-like oxidized LDL receptor-1. *Arterioscler. Thromb Vasc. Biol.* **20**, 715–720
30. Cooper, T.M. and Woody, R.W. (1990) The effect of conformation on the CD of interacting helices: a theoretical study of tropomyosin. *Biopolymers* **30**, 657–676
31. Zhou, N.E., Kay, C.M., and Hodges, R.S. (1992) Synthetic model proteins. Positional effects of interchain hydrophobic interactions on stability of two-stranded alpha-helical coiled-coils. *J. Biol. Chem.* **267**, 2664–2670
32. Kammerer, R.A., Schulthess, T., Landwehr, R., Lustig, A., Engel, J., Aebi, U., and Steinmetz, M.O. (1998) An autonomous folding unit mediates the assembly of two-stranded coiled coils. *Proc. Natl. Acad. Sci. USA* **95**, 13419–13424
33. Bain, A.D. (2003) Chemical exchange in NMR. *Prog. Nucl. Magn. Reson. Spectrosc.* **43**, 63–103
34. McLachlan, A.D. and Stewart, M. (1975) Tropomyosin coiled-coil interactions: evidence for an unstaggered structure. *J. Mol. Biol.* **98**, 293–304
35. Sodek, J., Dges, R.S.H., Smillie, L.B., and Jurasek, L. (1972) Amino-acid sequence of rabbit skeletal tropomyosin and its coiled-coil structure. *Proc. Natl. Acad. Sci. USA* **69**, 3800–3804
36. Kohn, W.D., Mant, C.T., and Hodges, R.S. (1997) Alpha-helical protein assembly motifs. *J. Biol. Chem.* **272**, 2583–2586
37. Li, Y., Brown, J.H., Reshetnikova, L., Blazsek, A., Farkas, L., Nyitray, L., and Cohen, C. (2003) Visualization of an unstable coiled coil from the scallop myosin rod. *Nature* **424**, 341–345
38. Li, Y., Mui, S., Brown, J.H., Strand, J., Reshetnikova, L., Tobacman, L.S., and Cohen, C. (2002) The crystal structure of the C-terminal fragment of striated-muscle alpha-tropomyosin reveals a key troponin T recognition site. *Proc. Natl. Acad. Sci. USA* **99**, 7378–7383
39. Steinmetz, M.O., Stock, A., Schulthess, T., Landwehr, R., Lustig, A., Faix, J., Gerisch, G., Aebi, U., and Kammerer, R.A. (1998) A distinct 14 residue site triggers coiled-coil formation in cortexillin I. *EMBO J.* **17**, 1883–1891
40. Segrest, J.P., Jones, M.K., De Loof, H., and Dashti, N. (2001) Structure of apolipoprotein B-100 in low density lipoproteins. *J. Lipid Res.* **42**, 1346–1367
41. De Loof, H., Rosseneu, M., Yang, C.Y., Li, W.H., Gotto, A.M., and Chan, L. (1987) Human apolipoprotein B: analysis of internal repeats and homology with other apolipoproteins. *J. Lipid Res.* **28**, 1455–1465
42. Lauzon, A.M., Fagnant, P.M., Warshaw, D.M., and Trybus, K.M. (2001) Coiled-coil unwinding at the smooth muscle myosin head-rod junction is required for optimal mechanical performance. *Biophys. J.* **80**, 1900–1904
43. Cambi, A., de Lange, F., van Maarseveen, N.M., Nijhuis, M., Joosten, B., van Dijk, E.M., de Bakker, B.I., Fransen, J.A., Bovee-Geurts, P.H., van Leeuwen, F.N., Van Hulst, N.F., and Figdor, C.G. (2004) Microdomains of the C-type lectin DC-SIGN are portals for virus entry into dendritic cells. *J. Cell Biol.* **164**, 145–155